Effect of Crosslinking on the Secondary Relaxation in Polyvinylethylene

R. CASALINI, C. M. ROLAND

Chemistry Division, Naval Research Laboratory, Code 6120, Washington, DC 20375-5342

Received 2 November 2009; revised 1 December 2009; accepted 2 December 2009
DOI: 10.1002/polb.21925
Published online in Wiley InterScience (www.interscience.wiley.com).

ABSTRACT: The effect of network formation on the secondary (Johari–Goldstein) β-relaxation was investigated for polyvinylethylene (PVE). Crosslinking affects the segmental (α-) process in the usual fashion, the networks exhibiting slower and more temperature-sensitive dynamics. However, the effect on the β-process is the opposite. The secondary relaxation becomes faster and the activation energy slightly decreases with crosslinking. The strength of the intermolecular cooperativity governing the behavior of the α-process was assessed using the coupling model, with consistent results obtained from analysis of both the timescale separating the α- and β-relaxations and the activation energy for the latter. © 2010 Wiley Periodicals, Inc. J Polym Sci Part B: Polym Phys 48: 582–587, 2010

KEYWORDS: cooperative effects; crosslinking; dielectric relaxation; glass transition; glassy polymers

INTRODUCTION

The intrinsic disorder of polymers deriving from their chemical structure makes them facile glass formers. On cooling toward the glass transition temperature, T_g, the segmental relaxation time progressively increases by more than 10 decades, from nanoseconds to hours, with secondary relaxations generally becoming evident close to and below T_g. Secondary relaxations exhibit quite disparate properties, depending on whether they arise from independent motion of a pendant group or have their origin in the dynamics of the main chain.[1–5] The latter are referred to as Johari–Goldstein (JG) relaxations[6] and involve all atoms of the repeat unit (intermolecular degrees of freedom). There is considerable interest in understanding any relationship between the properties of the JG and primary glass transition relaxation.[7–9] For example, on increasing hydrostatic pressure, the relaxation times of both the segmental and secondary relaxations of polymers increase, although the effect of pressure is strongest for the segmental mode[10,11] and weakest for the non-JG secondary relaxations.[1,5,12]

Crosslinking of polymers slows down the segmental dynamics, as reflected in an increased glass transition temperature.[13–20] For the case of polyvinylethylene (PVE), the effect of crosslinking on the segmental dynamics is typical: crosslinks broaden the dispersion in the mechanical and dielectric loss spectra and make the segmental relaxation time, τ_α, more sensitive to temperature (more "fragile").[21] Moreover, the dynamics become more sensitive to thermal energy relative to the effect of volume, as seen in the larger ratio of the isochoric and the isobaric activation energies.[22] In this work, we examine how the presence of a network affects the secondary relaxation in PVE. This polymer is well suited to such a study, because the secondary relaxation is a JG process that, while having a weak dielectric intensity, can be easily resolved from the segmental relaxation.

EXPERIMENTAL

The PVE was 96% 1,2-polybutadiene (the residual being the 1,4-addition product) obtained from Bridgestone Americas and having a weight average molecular weight = 153 kg/mol. Either 0.444 or 0.666% by weight dicumyl peroxide (DCP) crosslinker (Varox DCP-R from the R.T. Vanderbilt Co., Norwalk, CT) was added to cyclohexane solutions of the polymer. After drying, networks were prepared by curing for 30 min at 150 °C under pressure (the latter to avoid bubble formation). The networks are designated herein as PVE_1 and PVE_2; the network chain lengths, determined from the elastic modulus,[21] are listed in Table 1. For the case of PVE, the DCP liberates a hydrogen from a backbone carbon, creating a free radical that reacts with a carbon from another chain to form a covalent crosslink. The reaction propagates to yield junctions having high functionality (>4). As these crosslinks are carbon–carbon bonds, their dipole moment is negligible.

The temperature dependences of the relaxations were measured by dielectric spectroscopy using a Imass time domain spectrometer (10^{-4}–10^3 Hz), a Novocontrol Alpha High Resolution Impedance Analyzer (10^{-2}–10^6 Hz), and an Andeen-Hagerling Capacitance Bridge 2700A (50–2×10^4 Hz). The Andeen-Hagerling analyzer has very high resolution (0.1 aF), allowing accurate measurements of the weak secondary peak. The sample was maintained between parallel capacitor plates in a closed-cycle helium cryostat under

Correspondence to: R. Casalini (E-mail: riccardo.casalini@nrl.navy.mil)
Journal of Polymer Science: Part B: Polymer Physics, Vol. 48, 582–587 (2010) © 2010 Wiley Periodicals, Inc.

TABLE 1 Local Segmental Relaxation Properties

	N^a	T_g (K)[b]	$\log(\tau_{\alpha\infty})$ (s)	B (K)	T_0 (K)	β_{KWW}[c]	m
PVE	(linear)	272 ± 1	−10.4 ± 0.1	688 ± 13	247.6 ± 0.3	0.46	140
PVE_1	28	282 ± 2	−9.6 ± 0.3	475 ± 53	264 ± 1	0.43	185
PVE_2	21	289 ± 4	−9.3 ± 0.8	358 ± 82	275 ± 2	0.40	237

[a] Number of monomer units per elastically active chain.
[b] $\tau_\alpha = 100$ s.
[c] From eq 5.

vacuum, with temperature measured by a platinum resistance thermometer mounted in one of the electrodes.

RESULTS

The dielectric loss spectra of PVE (Fig. 1) at various temperatures reveal the presence of two relaxation processes, the α-process prominent above the glass transition and the β-process of much smaller intensity, well resolved in the spectra below the glass transition. The dielectric α-relaxation of PVE can be described by the one-sided Fourier transform of the Kohlrausch–Williams–Watts (KWW) correlation function[23,24] (solid lines in Fig. 1)

$$\Phi(t) = \exp\left[-(t/\tau_{KWW})^{\beta_{KWW}}\right] \quad (1)$$

where β_{KWW} ($0 < \beta_{KWW} \leq 1$) is the stretching exponent and τ_{KWW} a relaxation time. The α-process tends to became broader with decreasing temperature, reflected in the decrease of β_{KWW} for longer τ_{KWW} Fig. 1). The relaxation time, τ_{KWW}, is approximately equal to the τ_α defined from the reciprocal of the peak frequency ($\tau_{KWW}/\tau_\alpha = 0.7$ for the spectra herein).

The dielectric loss spectra for the two PVE networks (Figs. 2 and 3) show a similar behavior with the α, evident above T_g and the β-process resolved below T_g. In these two cases, however, the α-process is much broader and a KWW function cannot fit the α-peak, especially at low frequency, as seen in the deviation from the KWW fits (solid lines).

Thus, the α-peak in the dielectric spectrum of PVE shows the expected behavior,[21,22] broadening with increasing crosslinking and τ_α becoming more sensitivity to temperature. These relaxation times (defined as the reciprocal of the frequency of the α-loss peak maximum) are plotted in Figure 4, along with fits to the Vogel–Fulcher–Tamman–Hesse (VFTH) equation[25]

$$\tau_\alpha(T) = \tau_\infty \exp\left(\frac{B}{T - T_0}\right) \quad (2)$$

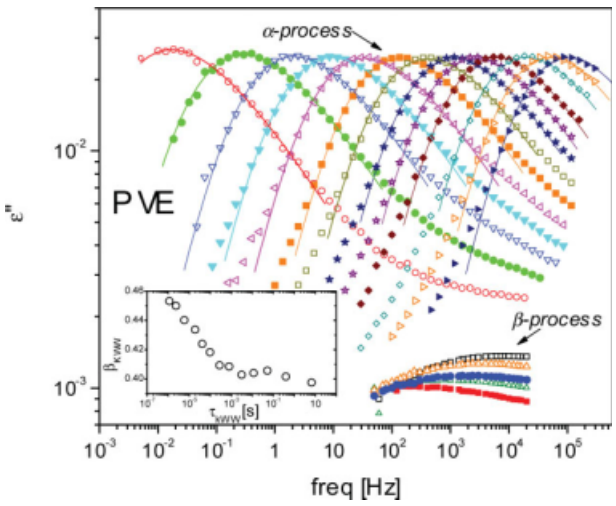

FIGURE 1 Dielectric loss spectra of linear PVE. Above the glass transition only the α-process is clearly resolved, the β-process becoming evident below the glass transition due to its weaker T-dependence. The temperatures are from right to left above T_g: 309.9, 306.1, 302.0, 297.3, 294.6, 292.0, 289.1, 286.5, 283.8, 281.3, 276.5, 273.7, 279.0 K, and below T_g: 254.3, 245.1, 236.8, 229.4, 215.9 K. The solid lines are the best fit to the KWW relaxation function eq 1. The inset shows the stretch exponent, β_{KWW}, determined by direct fitting of the α-peak using the KWW. [Color figure can be viewed in the online issue, which is available at www.interscience.wiley.com.]

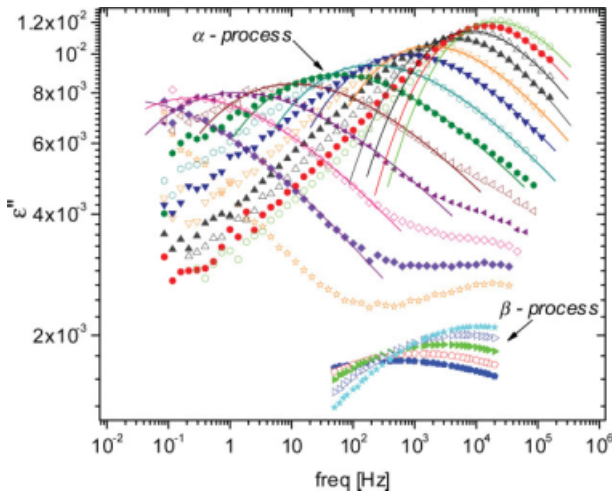

FIGURE 2 Dielectric loss spectra of PVE_1. Similar to linear PVE, the α-process is only resolved above the glass transition, the β-peak emerging at lower temperatures. The temperatures are from right to left above T_g: 310.0, 308.2, 306.1, 303.7, 301.3, 298.9, 296.1, 293.5, 290.9, 288.1, 285.7, 280.9, and below T_g: 256.6, 248.3, 239.1, 230.0, 222.1 K. The solid lines are the fit of the high frequency side of the α-process to the KWW relaxation function eq 1; the function deviates on the low frequency side of the peak. For this approximate fitting, the β_{KWW} varies from 0.29 to 0.19 from high to low temperature. [Color figure can be viewed in the online issue, which is available at www.interscience.wiley.com.]

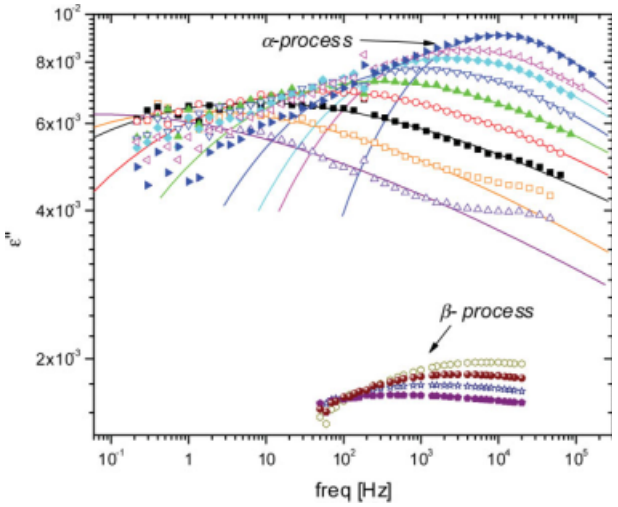

FIGURE 3 Dielectric loss spectra of PVE_2. The behavior of the more crosslinked network is similar to that in Figure 2. The temperatures are from right to left above T_g: 309.4, 306.1, 304.5, 302.5, 300.3, 298.1, 295.8, 293.4, and below T_g: 241.9, 232.5, 224.1, 215.9 K. The solid lines are fits of the high frequency side of the α-process to the KWW function eq 1, with large deviations apparent on the low frequency side of the peak. The β_{KWW} exponent varies from 0.25 to 0.12 from high to low temperature.

where τ_∞ is the high temperature limiting value of the relaxation time, and B and T_0 are constants (the latter sometimes referred to as the Vogel temperature). The best-fit parameters are given in Table 1 for the three samples.

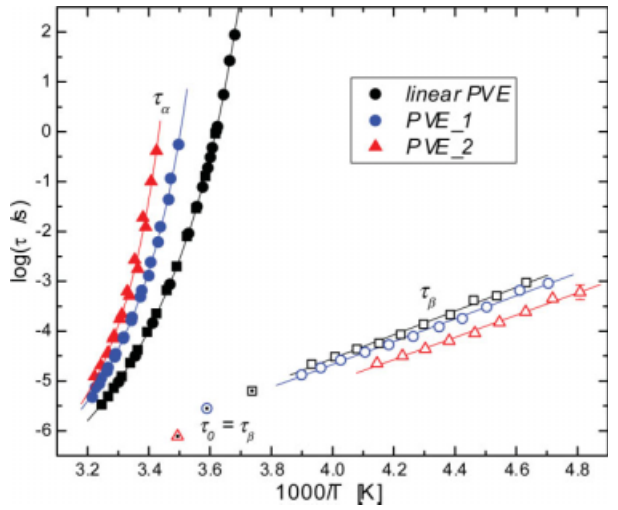

FIGURE 4 Relaxation map. Relaxation times for the local segmental (filled symbols) and secondary (open symbols) processes in linear and crosslinked PVE. Solid lines are the best-fit of the VFT equation for the α-relaxation process and the Arrhenius equation for the β-process. The errors that are smaller than the symbols were not shown. The open symbols with dotted center denote the location on the relaxation map at which $\tau_\beta = \tau_0$, obtained by extrapolating $\tau_\beta(T)$ to the temperature at which for $\tau_\alpha = 3.5 \times 10^4$ s for each sample.

At any given temperature, the local segmental relaxation time t_α increases several orders of magnitude due to crosslinking. This slowing down of the segmental dynamics is also manifested as an increase in T_g, by as much as 17 K for the more crosslinked sample (Table 1). Similar results were obtained by calorimetry[21] and volumetric measurements.[22] A metric of the T-dependence of τ_α is the steepness index or fragility, $m = \frac{d\log(\tau_\alpha)}{d(T_g/T)}\Big|_{T=T_g}$, which is the apparent activation energy at T_g normalized by thermal energy. The fragility calculated from the VFTH parameters are listed in Table 1. These are very high and consistent with previous results from mechanical[26–28] and dielectric[21] experiments. PVE is one of the most fragile amorphous polymers, with m for the networks close to the upper limit observed for any glass-forming material.[29–32]

Because of its much lower dielectric strength, the β-peak can only be resolved below T_g, where dielectric losses due to the segmental dynamics fall outside the measured frequency range. Interestingly, the introduction of a network has an opposite effect on the β-dynamics than on the segmental relaxation; to wit, crosslinking speeds up the β-process. For example, τ_α for PVE_2 is 3.5 decades longer than τ_α for the linear

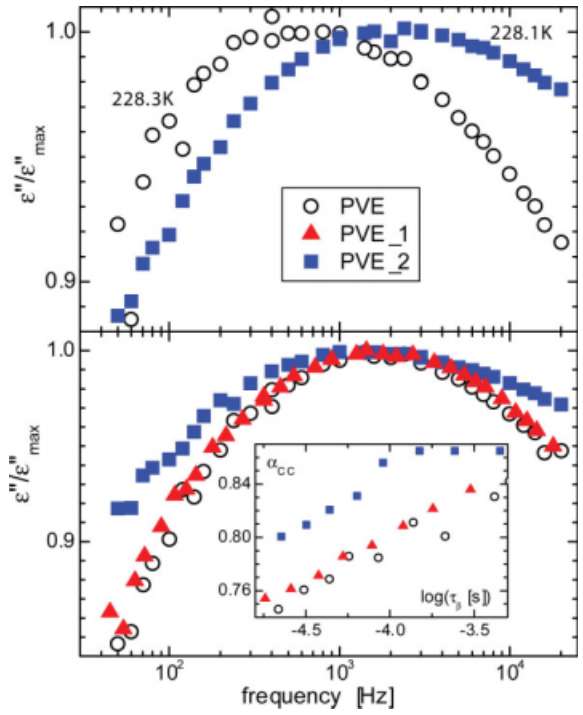

FIGURE 5 (Top) β-relaxation peak in the dielectric loss measured at the indicated temperatures for linear and the more crosslinked PVE. The latter is at higher frequency even though it was measured at slightly (0.2 K) lower temperature. (Bottom) Dielectric β-loss peaks of the linear PVE (236.0K), PVE_1 (234.6K), and PVE_2 (223.0K), showing the broadening with increased crosslinking (abscissa values for PVE_1 were shifted by 0.9 to make the maxima coincide). The insert is the fitted shape parameter for the Cole-Cole distribution function as a function of the β-relaxation time.

TABLE 2 Johari–Goldstein Relaxation Properties

	τ_β (T_g)	$\log(\tau_{\beta\infty})$ (s)	E_β (kJ/mol)	E_β (kJ/mol)[a]	n
PVE	−5.20	−14.1 ± 0.3	45.6 ± 1	45.3 ± 1	0.54
PVE_1	−5.55	−13.9 ± 0.2	44.0 ± 1	43.7 ± 1	0.57
PVE_2	−6.11	−13.9 ± 0.3	42.7 ± 1	42.5 ± 2	0.60

[a] From eq 6.

PVE; however, the β-relaxation time, τ_β, of the network is about threefold faster. This result is illustrated in Figure 5 (top), showing representative β-relaxation peaks for the linear PVE and PVE_2; the peak maximum for the network is at a higher frequency.

The secondary relaxation times conformed to the Arrhenius function

$$\tau_\beta(T) = \tau_{\beta\infty} \exp\left(E_\beta/RT\right) \tag{3}$$

the fits to which are included in Figure 4, with the fit parameters listed in Table 2. The high temperature limiting value, $\tau_{\beta\infty}$, is independent of crosslinking (within the experimental error), while there is a small decrease of the activation energy, E_β, for the networks. Kudlik et al.[33] suggested the relation $E_\beta = 24\ RT_g$, but herein, we find $E_\beta/RT_g = 20.2 \pm 0.5$, 18.8 ± 0.5, and 17.8 ± 0.5 for the linear PVE, PVE_1, and PVE_2, respectively.

The β-relaxation spectra for the three samples can be described by the symmetric Cole–Cole function[34]

$$\varepsilon^*(2\pi f) = \varepsilon_\infty + \Delta\varepsilon_\beta/\left(1 + i2\pi f\tau_\beta\right)^{1-\alpha_{CC}} \tag{4}$$

where ε_∞ is the high-frequency permittivity, $\Delta\varepsilon_\beta$ the dielectric strength, and α_{CC} a shape parameter. As seen in Figure 5, the breadth of the β-peak increases with crosslinking, with the effect more pronounced for the more crosslinked network. The broadening of the α-process with crosslinking is not the same as the broadening of the β-peak, because the latter remains symmetric; whereas the α-relaxation is affected primarily at lower frequencies.

DISCUSSION

The behavior of the β-process in PVE is unexpected. Crosslinking increases the mass density (by about 5% herein) and the general expectation is that densification, similar to hydrostatic pressure, will increase relaxation times due to greater crowding. A 5% increase of volume below T_g corresponds to a pressure increase of about 100 MPa,[22] and therefore, the change in τ_β observed for the PVE networks corresponds to an activation volume, $\left(\equiv RT\frac{d\log\tau_\beta}{dP}\right)$ of about -23 cm^3/mol. Note, there is no precedent for a negative activation volume in polymers or molecular liquids.

The coupling model (CM) of Ngai[35–37] relates the strength of the intermolecular cooperativity governing the α-relaxation to properties of the JG β-relaxation, specifically the temporal separation between the two processes and the activation energy of τ_β. At T_g, the timescale separating the α- and β-processes has been found to be correlated with the stretch exponent β_{KWW} of the α-process as defined in eq 1 [see ref. 38].

The KWW function eq 1 cannot be applied directly to the measured α-peaks for the networks, because this equation and the CM interpretation of β_{KWW} only account for statistical variations in the relaxation rate among segments due to their presence in dense phase. There is an additional contribution to the broadening due to the inhomogeneity of the local environment in the crosslinked samples; the local α-dynamics vary with proximity of a segment to a network junction. Such an effect is severe in PVE networks, given the high functionality of the crosslinks.[39] This broadening is dominant on the low frequency side of the α-peak, causing deviation from the KWW shape (Figs. 2 and 3).

According to the CM, there is a relationship between the α- and β-relaxation times.

$$\log\left(\tau_\beta\right) = (1-n)\log(\tau_\alpha) + n\log(t_c) \tag{5}$$

where t_c is a temperature-independent time constant equal to 2 ps.[35,36] In this equation, n is the coupling parameter characterizing the strength of the intermolecular constraints on the α-process. For homogeneously broadened spectra, $n = 1 - \beta_{KWW}$, so that the coupling parameter is obtained directly from the spectra. However, for networks, in which segments have varying dynamics depending on their proximity to a junction, n cannot be determined from fitting the peaks. Previously[21] we made the assumption that the JG process is unaffected by crosslinking and deduced n as the values for which eq 5 yields constant τ_β; that is, τ_β is independent of crosslinking at any given temperature.

This assumption is unnecessary herein, because the JG secondary relaxation times are measured (and indeed, the data in Fig. 4 indicate an effect of crosslinking on τ_β). Instead, we determine the value of n in eq 5 yielding the experimentally determined τ_β. This calculation is carried out at the temperature for which $\tau_\alpha = 3.5 \times 10^4$ s, since the segmental process ceases in the glassy state. The values of τ_β at T_g are obtained by extrapolation using eq 3. These results, summarized in Table 2, again indicate the anomalous speeding up of the JG secondary relaxation due to crosslinking, when compared with T_g. The value determined for n are consistent with enhanced intermolecular cooperativity due to crosslinking, which contributes to the broadening of the α-peak.

An additional prediction of the CM is that the activation energy for the secondary relaxation, E_β, is related to the properties of the α-relaxation according to the following equation[40]:

$$E_\beta = 2.303RT\left[(1-n)\log(\tau_\alpha) + n\log(t_c) - \log\left(\tau_{\beta\infty}\right)\right] \tag{6}$$

This equation provides a means to corroborate the analysis using eq 5, coupling parameters determined using eq 5, we

apply eq 6 to each sample at the respective temperature for which $\tau_\beta = \tau_0$. The results are listed in Table 2, where the calculated activation energies are seen to be within the uncertainty of measured values. This affirms both the CM analysis and the weak decrease observed for E_β with crosslinking.

Finally, we note our recent finding[41] that in polymer glasses formed along different thermodynamic pathways, the timescale of the β-process reflects the local (<0.5 nm) density fluctuation of the glass. Thus, glasses having smaller local density fluctuations, such as aged glasses, have faster β-processes than glasses with larger local density fluctuations, such as pressure-densified glasses. As suggested in the earlier work[41] and herein, networks are another means to reduce τ_β, because the constraints from the crosslinks on local segmental motions are expected to reduce the amplitude of the local density fluctuations. The expectation of a relationship between the local density fluctuations and the failure properties of glasses makes this an intriguing area for future work. Although a firm theoretical justification remains to be developed, intuitively the changes of intermolecular cooperativity (n) and the intensity of local density fluctuations should be correlated, because both reflect the probability of segmental rearrangements.

CONCLUSIONS

Dielectric spectroscopy was used to study the JG secondary relaxation in linear and crosslinked PVE. The local segmental dynamics are affected in the usual way by crosslinking the α-peak moving to lower frequencies and becoming broader. This increased breadth has two origins, enhanced intermolecular cooperativity, and an inhomogeneous broadening due to the difference in relaxation times for segments close to and far from the network junctions. The behavior of the secondary process in the networks is anomalous. Crosslinking makes the β-relaxation faster, even though the T_g is higher than for linear PVE. The networks are also more fragile (m is among the largest found for any material), yet have a smaller activation energy for τ_β Although, in general, β-processes are less sensitive to structural and thermodynamic variables than the α-relaxation, the secondary relaxation behavior of the PVE networks is counter-intuitive. The additional constraints and greater density resulting from crosslinking are not expected to give rise to faster and less temperature-sensitive dynamics.

The authors thank Terry Hogan of Bridgestone Americas for synthesizing the polymer. This work was supported by the Office of Naval Research.

REFERENCES AND NOTES

1 Lunkenheimer, P.; Loidl, A. Chem Phys 2002, 284, 205–219.

2 Mierzwa, M.; Pawlus, S.; Paluch, M.; Kaminska, E.; Ngai, K. L. J Chem Phys 2008, 128, 044512.

3 Mandanici, A.; Huang, W.; Cutroni, M.; Richert, R. J Chem Phys 2008, 128, 124505.

4 Casalini, R.; Roland, C. M. Phys Rev Lett 2003, 91, 015702.

5 Ngai, K. L. J Phys: Cond Matt 2003, 15, S1107–S1125.

6 (a) Johari, G. P.; Goldstein, M. J Phys Chem 1970, 74, 2034–2035; (b) Johari, G. P.; Goldstein, M. J Chem Phys 1970, 53, 2372–2388.

7 Prevosto, D.; Capaccioli, S.; Lucchesi, M.; Rolla, P. A.; Ngai, K. L. J Non-Cryst Solids 2009, 355, 705–711.

8 Lunkenheimer, P.; Pardo, L. C.; Koehler, M.; Loidl, A. Phys Rev E 2008, 77, 031506.

9 Buchenau, U. J Non-Cryst Solids 2007, 353, 3812–3819.

10 Roland, C. M.; Hensel-Bielowka, S.; Paluch, M.; Casalini, R. Rep Prog Phys 2005, 68, 1405–1478.

11 Kessairi, K.; Capaccioli, S.; Prevosto, D.; Lucchesi, M.; Sharifi, S.; Rolla, P. A. J Phys Chem B 2008, 112, 4470–4473.

12 Casalini, R.; Roland, C. M. Phys Rev B 2005, 69, 094202.

13 Mangion, M. B. M.; Johari, G. P. J Polym Sci Polym Phys Ed 1991, 29, 1127–1135.

14 (a) Mijovic, J.; Han, Y. F.; Sun, M. Y.; Pejanovic, S. Macromolecules 2003, 36, 4589–4602; (b) Mijovic, J.; Fishbain, A.; Wijaya, J. Macromolecules 1992, 25, 986–989; (c) Meyer, F.; Sanz, G.; Eceiza, A.; Mondragon, I.; Mijovic, J. Polymer 1995, 36, 1407–1414.

15 Roland, C. M.; Santangelo, P. G.; Antonietti, M.; Neese, M. Macromolecules 1999, 32, 2283–2287.

16 Tonpheng, B.; Andersson, O. Eur Polym J 2008, 44, 2865–2973.

17 Duenas, J. M. M.; Mateo, J. M.; Ribelles, J. L. G. Polym Eng Sci 2005, 45, 1336–1342.

18 (a) Tombari, E.; Salvetti, G.; Johari, G. P. J Chem Phys 2000, 113, 6957–6965; (b) Cardelli, C.; Tombari, E.; Johari, G. P. J Phys Chem B 2001, 105, 11035–11043.

19 Casalini, R.; Corezzi, S.; Livi, A.; Levita, G.; Rolla, P. A. J Appl Polym Sci 1997, 65, 17–25.

20 Friedrich, K.; Ulanski, J.; Boiteux, G.; Seytre, G. Polimery 2006, 51, 264–269.

21 Roland, C. M. Macromolecules 1994, 27, 4242–4247.

22 (a) Roland, C. M.; Roland, D. F.; Wang, J.; Casalini, R. J Chem Phys 2005, 123, 204905; (b) Roland, C. M.; Roland, D. F.; Wang, J.; Casalini, R. J Chem Phys 2008, 129, 179902.

23 Kohlrausch, R. Ann Phys 1847, 12, 393–398.

24 Williams, G.; Watts, D. C. Trans Faraday Soc 1970, 66, 80–85.

25 Ferry, J. D. Viscoelastic Properties of Polymers; Wiley: New York, 1980.

26 Roland, C. M.; Ngai, K. L. Macromolecules 1991, 24, 5315–5319.

27 Zorn, R.; McKenna, G. B.; Willner, L.; Richter, D. Macromolecules 1995, 28, 8552–8562.

28 Robertson, C. G.; Rademacher, C. M. Macromolecules 2004, 37, 10009–10017.

29 Böhmer, R.; Ngai, K. L.; Angell, C. A.; Plazek, D. J. J Chem Phys 1993, 99, 4201–4209.

30 Ngai, K. L.; Plazek, D. J. Macromolecules 1991, 24, 1222–1224.

31 Huang, D.; McKenna, G. B. J Chem Phys 2001, 114, 5621–5630.

32 Note that the values of *m* reported in ref. 7 are low by a factor of 2.3 due to a calculation error.

33 Kudlik, A.; Tschirwitz, C.; Benkhof, S.; Blochowicz, T.; Rössler, E. Europhys Lett 1997, 40, 649–654.

34 Cole, K. S.; Cole, R. H. J Chem Phys 1941, 9, 341–351.

35 Ngai, K. L.; Rendell, R. W. ACS Symp Ser 1997, 676, 45–66.

36 Ngai, K. L.; Tsang, K. Y. Phys Rev E 1999, 60, 4511–4517.

37 Ngai, K. L.; Roland, C. M. Macromolecules 1993, 26, 6824–6830.

38 Ngai, K. L. Phys Rev E 1998, 57, 7346–7349.

39 Roland, C. M. In Science and Technology of Rubber; Mark, J. E.; Erman, B.; Eirich, F. R., Eds.; Elsevier: New York, 2005.

40 Ngai, K. L.; Capaccioli, S. Phys Rev E 2004, 69, 031501.

41 Casalini, R.; Roland, C. M. J Chem Phys 2009, 131, 114501.